

# 灭菌器组合工艺焊接残余应力的消除与评价

张亦良<sup>1</sup>, 刘金艳<sup>1</sup>, 赵尔冰<sup>2</sup>, 徐学东<sup>1</sup>, 程红伟<sup>2</sup>

(1. 北京工业大学 机电学院, 北京 100124; 2. 北京市朝阳区特种设备检测所, 北京 100021)

**摘 要:** 针对国产脉动真空灭菌器内腔焊缝处多次开裂现象, 围绕焊接残余应力及消除方法进行了系列研究. 根据市场上灭菌器异种钢间断角焊缝特征设计了7种组合结构焊板, 应用X射线法定量给出了残余应力分布规律, 并对用焊后浇水速冷处理工艺消除残余应力的尝试进行了试验验证. 结果表明, 各种焊板残余应力均达到屈服应力, 由此引起的应力腐蚀与腐蚀疲劳是灭菌器内腔开裂的直接原因; 二氧化碳焊接工艺残余应力较焊条电弧焊高10%~22%, 残余应力与加强筋类型基本无关; 浇水速冷处理工艺可有效降低表面残余应力, 降幅达50%~70%, 提高疲劳极限12%~14%. 有效降低焊接残余应力是解决内腔开裂的重要途径.

**关键词:** 焊接; 残余应力; X射线法; 灭菌器; 裂纹

**中图分类号:** TB301, TG113.26 **文献标识码:** A **文章编号:** 0253-360X(2009)10-0097-05



张亦良

## 0 序 言

脉动真空灭菌器是医疗等行业消毒的主要设备<sup>[1]</sup>, 其内腔为蒸汽灭菌空间, 用于放置被灭菌物品. 内腔通入蒸汽加热进行灭菌, 使用中内腔经利抽真空、加热、灭菌、干燥等工作过程, 在夹套蒸汽的外压下承受多次压力波动.

目前国产灭菌器面临的主要问题是使用一段时间后即发生内腔大量开裂导致早期报废, 据272台注册灭菌器的统计, 能够使用3年以上的只有132台, 仅占49%(进口灭菌器一般使用寿命均在12年以上). 对17台灭菌器跟踪监测, 14个月后9台(全部为脉动真空类型)已经开始泄漏, 裂纹均分布在加强筋与内壁焊缝周边. 为寻找开裂原因曾进行了系列检验, 金相及断口分析表明裂纹为解理状穿晶断裂, 均从内壁起裂, 具有典型的应力腐蚀裂纹特征. 造成应力腐蚀有两大因素: 一是腐蚀环境, 这是灭菌工作性质所决定的; 二是应力, 由工作应力及焊接残余应力叠加而成. 对工作应力的测试表明, 1.5倍的使用压力下, 其动、静态最大应力仅为 $0.21\sigma_s$ <sup>[1,2]</sup> (该应力水平不足以引起应力腐蚀, 屈服极限 $\sigma_s = 297$  MPa), 焊接残余应力为主要矛盾. 从灭菌器的使用现状看, 采取有效的工艺措施对焊接残余应力进行控制和消除, 具有重要的实际意义<sup>[3]</sup>.

对于焊接残余应力的产生与消除, 诸多学者已做过大量基础性研究, 文献[4-6]对焊接残余应力的产生机理和消除方法进行探讨, 从不同角度针对理想模型做出分析, 引入了固有应变的概念. 但是按照实际多种焊接工艺产生的残余应力, 其量值、分布以及消除方法远比理想模型复杂得多, 如温差处理法处理前后残余应力沿厚度方向的分布规律、多层多道焊、焊缝长度及焊接方向、间断角焊缝起弧收弧点、异种材料焊接残余应力的分布规律等则非常复杂. 在锅炉压力容器、管道领域中, 对于奥氏体不锈钢、钛铝等有色金属残余应力的控制与消除一直未能较好解决, 对其深入研究需要大量试验分析<sup>[7,8]</sup>.

文中在对国内外灭菌器设计、制造和使用做全面调研的基础上, 对实际生产中经常使用的异种钢间断角焊缝应用X射线法<sup>[9-12]</sup>做了多种组合结构的残余应力测定, 给出了定量评价及分布规律; 在此基础上, 尝试应用浇水速冷处理工艺消除残余应力. 通过大量的实测结果, 明确了该工艺对焊接残余应力的影响程度, 为寻求灭菌器更加适宜的焊接方式及制造工艺提供试验依据.

## 1 试验方法

### 1.1 试验材料及焊接方式

灭菌器的夹层空间厚度为50 mm左右, 为加强

刚度,焊有型钢作为拉撑加固(夹层焊接结构见图1),在灭菌器内腔焊接结构的生产过程中,不同生产厂家具有以下几个特点:(1)应用材料基本是0Cr18Ni9(304)不锈钢,但供货来源不同;(2)采用了不同的焊接方式及工艺(包括不同的焊缝长度);(3)采用了不同的拉撑加强筋类型(包括角钢、槽钢及钢带)。

试验选择 304 不锈钢,考虑 3 个国家的供货渠道,采用 7 种不同的焊接方式,面内尺寸均为 500 mm×400 mm. 焊接方式见表 1,力学性能见表 2.



图 1 夹层焊接结构图

Fig 1 Welded Inner Frame

表 1 焊接方式  
Table 1 Welding methods

材料产地	编号	板厚 $a/mm$	焊接方法		焊缝形式			加强筋		速冷工艺
			焊条电弧焊	CO <sub>2</sub> 焊	长缝	短缝	对接	钢带	槽钢	
韩国	1	4	✓			✓		✓		
	2	4	✓		✓			✓		
	3	4	✓		✓				✓	
	4	5		✓	✓			✓		
	5	5		✓		✓		✓		
德国	6	6	✓				✓			✓
宝钢	7	6	✓				✓			✓

表 2 材料力学性能

Table 2 Mechanical properties of materials

材料产地	下屈服强度 $R_{eL}/MPa$	抗拉强度 $R_m/MPa$	断后伸长率 $A(\%)$
韩国	297	688	52.0
德国	376	667	39.1
宝钢	346	681	41.9

1.2 焊接工艺

焊条电弧焊:焊条为  $\phi 4.0$  mm 的 A302 不锈钢焊条,焊接电流为 125 A,电弧电压为 20~30 V,焊接速度为 200 mm/min.

二氧化碳(CO<sub>2</sub>)保护焊:采用  $\phi 1.0$  mm 的 EL308 不锈钢药芯焊丝,焊接电流为 150 A,电弧电压为 20~30 V,焊接速度为 300 mm/min.

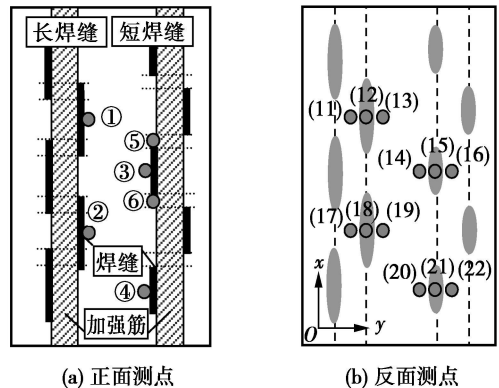
焊后浇水速冷处理工艺:双面焊接,第 1 次正常焊,第 2 次将板翻转 180° 焊.焊接过程分段浇水,浇水时焊板温度为 900~1 050 °C,浇水范围为焊缝四周各 60 mm 左右,浇水水温为 20 °C±2 °C.

1.3 测试仪器

日本理学 MSF-2M 型 X 射线应力仪.特性谱线 Cr-K $\beta$ ;测试晶面 (311) 面;X 光管工作电压 30 kV;X 光管工作电流 6~8 mA;固定  $\Psi_0$  法, $\Psi_0$  站选为 0°, 15°, 30°, 45°<sup>[13]</sup>.

1.4 残余应力测试方案

模拟灭菌器内腔的拉撑焊接工艺特点(夹层面拉撑采用不同长度的间断焊接),将两条不同形式拉撑板焊接在试板一面,采用长(焊缝有重叠)、短(无重叠)焊缝(图 2).两种焊接工艺下焊接不同拉撑板:①焊接 500 mm×40 mm×3mm 钢带(长焊缝、短焊缝);②焊接 No.5 槽钢.重点测试焊缝及热影响区,比较各工艺优劣.规定平行焊缝方向为  $x$  向,焊接面为正面.



(a) 正面测点

(b) 反面测点

图 2 典型焊板残余应力测点布置

Fig. 2 Measuring points layout of residual stress

1.5 残余应力测点布置

考虑到裂纹均从内壁(焊接背面)起裂的特点,

重点测试焊板反面应力, 典型焊板残余应力测点布置见图 2。浇水速冷处理工艺中采用对接焊及焊接槽钢, 对焊板一半浇水, 定义最后浇水面为“正面”, 浇水侧为 AA 线, 原始焊态(未浇水)为 BB 线。反面相应测点为 A'A' 及 B'B', 见图 3。

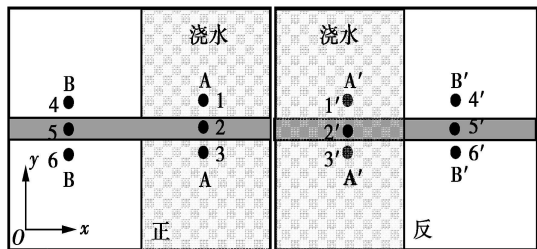


图 3 焊后浇水板测点布置

Fig 3 Measuring points layout of post-weld watering plate

## 2 两种焊接工艺测试结果及分析

### 2.1 焊条电弧焊接的残余应力

焊条电弧焊的 3 种焊板残余应力综合比较见表 3。

表 3 焊条电弧焊残余应力测试综合结果

Table 3 Residual stress test comprehensive results of shielded metal arc welding plate

焊缝	焊缝金属残余应力 $\sigma_1$ /MPa		热影响区残余应力 $\sigma_2$ /MPa	
	平均值	最大值	平均值	最大值
短焊缝 1 号	246	262	213	260
长焊缝 2 号	193	233	233	297
相差幅度(%)	27	12	-9.40	-14
槽钢 3 号	166	233	219	297

焊接残余应力的最大值出现在长焊缝焊板热影响区处为 297 MPa, 相当于  $1.0 \sigma_s$  (按试板材料实测屈服极限  $\sigma_s = 297$  MPa 计算), 平均值为  $0.74 \sigma_s$ 。该应力对于焊接试板而言, 已经是较高的应力水平。

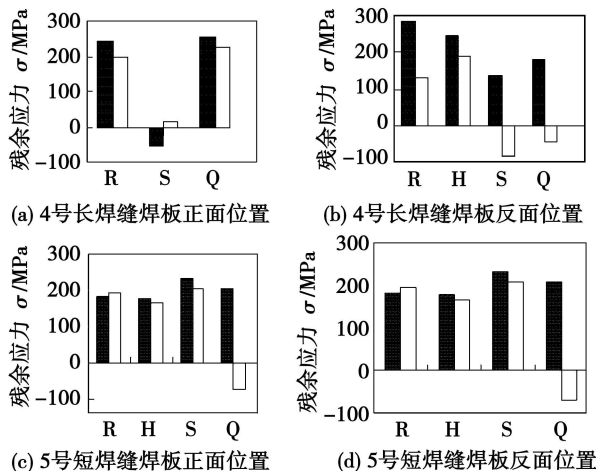
热影响区长焊缝的残余应力均值较短焊缝大 9.4%, 但焊缝金属上情况相反。仅从焊缝长度并未显示出明显规律。

槽钢加强筋板与钢带长焊缝板的应力分布基本相当。试验证明残余应力与加强筋的类型基本无关。

### 2.2 二氧化碳保护焊工艺的残余应力

长(4号)、短(5号)焊板与正(焊接面)、反面残余应力平均值综合比较见图 4。热影响区残余应力

最大, 4 号达  $1.09 \sigma_s$ , 平均值  $0.96 \sigma_s$ , 焊缝处最大值为  $0.83 \sigma_s$ 。4 号板较 5 号板焊缝金属及热影响区处残余应力分别大 21% 及 17%。x 向残余应力明显高于 y 向, 与焊接残余应力分布理论相吻合<sup>[14]</sup>。焊接起弧点较收弧点残余应力平均值大 84%。



R 为热影响区, H 为焊缝金属, S 为收弧点, Q 为起弧点  
■ x 向平行焊缝, □ y 向垂直焊缝

图 4 二氧化碳焊板残余应力平均值对比

Fig. 4 Stress comparison of CO<sub>2</sub> welding plate

### 2.3 两种焊接工艺残余应力对比

两种焊接工艺典型部位残余应力结果对比见图 5, 二氧化碳焊工艺残余应力平均值普遍高于焊条电弧焊, 从热影响区残余应力看, 长焊缝板高 22%, 短焊缝板高 10%。

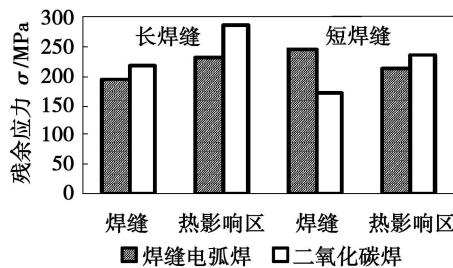


图 5 两种焊接方式残余应力平均值对比

Fig 5 Stress values contrast of two welding methods

### 2.4 裂纹发生于焊缝热影响区的成因分析

经大量检验发现, 应力腐蚀裂纹和疲劳裂纹大部分发生在焊缝热影响区。焊接接头由焊缝区、熔合及半熔合区、热影响区及母材组成。焊缝区在焊接和冷却过程中没有加热过程, 引起残余应力的拉伸弹性应变, 其数值为热收缩量与热收缩拉伸塑性应变之差。热影响区在焊接过程中经历了加热时的

热压缩塑性应变,冷却过程中经历了热收缩拉伸塑性应变和弹性应变,引起残余应力的拉伸弹性应变数值是压缩塑性应变与拉伸塑性应变之差.虽然两种情况数值上相同<sup>[9]</sup>,但原理不同,引起的后果不同.熔合线和热影响区在加热和冷却过程中温度梯度很大,是金相组织劣化区域.如果不考虑焊接缺陷的影响,熔合线和热影响区是最容易形成裂纹的部位.

从文中测试的7种结构焊板来看,最大残余应力均出现在焊缝热影响区部位,为平行焊缝方向.从灭菌器的实际检验中发现,大部分裂纹出现在热影响区处,为垂直焊缝方向.可见测试结果与传统焊接理论、裂纹缺陷形式相吻合.

### 3 焊后浇水速冷工艺的残余应力

#### 3.1 焊后浇水速冷工艺对残余应力的降低机制

浇水速冷实际上是温差法和逆焊接处理法的一种简易实用处理工艺<sup>[8,14,15]</sup>,是在焊接完成后,焊件温度在600℃以上时,在接触介质并存在应力腐蚀可能性的表面迅速浇水,以降低该面焊接残余应力的方法.其原理是利用急冷造成沿厚度方向不均匀的温度场,使该表面焊接区获得负温差,则在冷却收缩过程中由于内层金属的拘束而产生拉伸塑性变形,抵消焊接过程中形成的压缩塑性变形,达到降低该表面残余拉应力之目的.

#### 3.2 浇水速冷后残余应力平均值

浇水速冷工艺采用全焊透的对接焊,在焊板的一半进行浇水处理.6号(德国材料)正面(浇水面)浇水与未浇水(原始焊态)部分应力比较见表4及图6a.焊缝及热影响区平行焊缝方向的最大主应力 $\sigma_x$ (平均值)降低68%, $\sigma_y$ (平均值)降低了29%,可见浇水速冷可有效降低残余应力.

表4 6号板正面浇水与原始焊态残余应力对比

Table 4 Residual stress contrast of positive watering and original state for board 6

测试位置	y向应力			x向应力		
	浇水后 $\sigma_y$ /MPa	原始态 $\sigma_y$ /MPa	降幅 (%)	浇水后 $\sigma_x$ /MPa	原始态 $\sigma_x$ /MPa	降幅 (%)
热影响区	112	151	26	85	244	65
焊缝	192	338	43	79	284	72
平均降幅(%)		34.5			68.5	

#### 3.3 浇水速冷一侧正反两面残余应力

浇水侧正反两面残余应力平均值结果见图6b,由图6b可见,尽管浇水侧正面残余应力有较大幅度降低,但反面残余应力基本不受浇水的影响,说明此

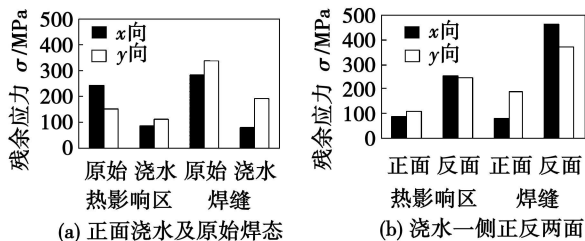


图6 焊后浇水速冷残余应力平均值比较

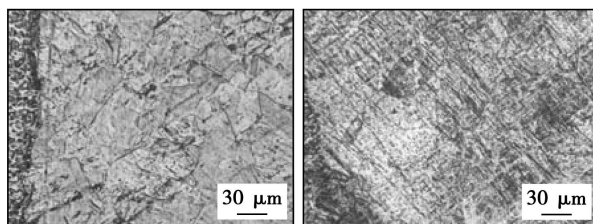
Fig 6 Comparison of residual stress values by post-weld watering

工艺只能有效降低浇水侧表面的残余应力.

#### 3.4 浇水速冷工艺处理后的金相组织

图7a示出原始焊态的金相组织为奥氏体,并有孪晶,该图显示距熔合线0~300μm处,热影响区处的晶粒尺寸为50~70μm.金相观察距熔合线1mm以外的母材处,晶粒尺寸为30~60μm.可见,热影响区的晶粒尺寸大于母材的晶粒尺寸.

图7b给出浇水速冷工艺后的金相组织,显示距离熔合线0~300μm的热影响区处,晶粒尺寸为70~100μm.距熔合线1mm以外的母材处,晶粒尺寸为50~60μm左右.可见,浇水后熔合线附近即热影响区晶粒有所长大,但远离焊缝处的母材与原始焊态基本相当.



(a) 原始焊态

(b) 浇水速冷后

图7 焊缝热影响区金相组织

Fig 7 Microstructure of weld heat affected zone

#### 3.5 浇水速冷工艺后材料的疲劳性能

每块焊板分为原始焊态及焊后浇水速冷态,按垂直焊缝方向取疲劳试样,分别测定5组不同工艺的疲劳曲线,为模拟实际工况取应力比 $R=0.5$ ,结果见表5,其中 $\sigma_{0.5}$ 表示在 $R=0.5$ , $N=10^7$ 周次循环时仍未断裂的应力最高值, $\sigma_b$ 为与该组疲劳试样材料对应的拉伸实测值,为应力极限.

经过浇水速冷处理工艺,德国材料疲劳极限比原始焊态提高了12%,宝钢材料则提高14%,疲劳极限分别达到0.86 $\sigma_b$ 及0.80 $\sigma_b$ .浇水速冷处理工

艺提高了材料的疲劳性能。

表 5 不同材料的疲劳极限

Table 5 Fatigue limits of different materials

材料产地	状态	应力比为 0.5 时的应力		与 $\sigma_b$ 比较
		$\sigma_{0.5}/\text{MPa}$	实测应力 $\sigma_b/\text{MPa}$	
韩国	A 焊缝	449	654	0.68
	B 焊缝	516	667	0.77
德国	C 焊后浇水	576	674	0.86
	D 焊缝	469	681	0.70
宝钢	E 焊后浇水	536	685	0.80

## 4 结 论

(1) 各种结构焊板的残余应力均达到  $1.0 \sigma_s$ , 最大应力出现在热影响区平行焊缝方向。

(2) 两种焊接方式中, 二氧化碳焊接残余应力平均值为大, 较焊条电弧焊高  $10\% \sim 22\%$ 。

(3) 两种焊接工艺中, 长焊缝热影响区处残余应力较大, 残余应力与加强筋类型无关。

(4) 焊后浇水速冷处理工艺能够有效降低焊板表面残余应力, 正面降幅可达  $50\% \sim 70\%$ , 并可提高疲劳极限  $12\% \sim 14\%$ 。

## 参考文献:

[1] 杜伟, 刘鹏飞, 郑津洋, 等. 矩形蒸汽灭菌器强度数值模拟与试验研究[J]. 压力容器, 2007, 24(10): 17-21.  
Du Wei, Liu Pengfei, Zheng Jinyang, et al. Numerical simulation and experimental study of strength of rectangular steam-heated sterilizer[J]. Pressure Vessel Technology, 2007, 24(10): 17-21.

[2] 张亦良, 肖尧, 徐威, 等. 灭菌器内腔开裂的宏观应力分析[J]. 北京工业大学学报, 2008, 34(增刊): 89-95.  
Zhang Yiliang, Xiao Yao, Xu Wei, et al. Stress analysis for sterilizer inner surface cracking[J]. Journal of Beijing University of Technology, 2008, 34(s): 89-95.

[3] 何小东, 张广成, 裴怡. D406A 高强钢焊接残余应力测试[J]. 焊接技术, 2005, 34(2): 50-51.  
He Xiaodong, Zhang Guangcheng, Pei Yi. Measurement of welding residual stress in high strength steel D406A[J]. Welding Technology, 2005, 34(2): 50-51.

[4] 王者昌. 关于焊接残余应力消除原理的探讨[J]. 焊接学报, 2000, 21(2): 55-58.  
Wang Zhechang. Discussion on the elimination principle of welding residual stress[J]. Transactions of the China Welding Institution, 2000, 21(2): 55-58.

[5] 汪建华, 路皓. 焊接残余应力形成机制与消除原理若干问题的讨论[J]. 焊接学报, 2002, 23(3): 75-79.  
Wang Jianhua, Lu Hao. Welding residual stress formation mechanism and discussion of a number of issues on elimination principle[J].

Transactions of the China Welding Institution, 2002, 23(3): 75-79.

[6] 游敏, 郑小玲, 余海州. 关于焊接残余应力形成机制的探讨[J]. 焊接学报, 2003, 24(2): 51-56, 58.  
You Min, Zheng Xiaoling, Yu Haizhou. Discussion on welding residual stress formation mechanism[J]. Transactions of the China Welding Institution, 2003, 24(2): 51-56, 58.

[7] 陈积光, 豆志武, 赖伟栋, 等. 焊接钛制压力容器残余应力的研究[J]. 焊接技术, 2001, 30(2): 40-41.  
Chen Jiguang, Dou Zhiwu, Lai Weidong, et al. The residual stress research of welding titanium pressure vessel[J]. Welding Technology, 2001, 30(2): 40-41.

[8] 龙昕, 汪建华. 温差法在焊接残余应力和变形控制中的应用[J]. 压力容器, 2000, 17(4): 37-40.  
Long Xi, Wang Jianhua. A review of the application of forced chilling in controlling of residual stresses and distortion of welding[J]. Pressure Vessel Technology, 2000, 17(4): 37-40.

[9] Bahadur A, Ravi kumar B, Kumara S. Development and comparison of residual stress measurement on welds by various methods[J]. Materials Science and Technology, 2004, 20(2): 261-269.

[10] Hornbach D J, Prevey P S. The effect of prior cold work on tensile residual stress development in nuclear weldments[J]. Transactions of the ASME, Journal of Pressure Vessel Technology, 2002, 124(3): 359-365.

[11] Huang H R, Zhang Y L, Wang Q M. Measurement and analysis of surface residual stress of railroad wheels with X-ray method[C] // Proceedings of the 7th International Conference on Residual Stresses: Residual Stresses VII, ICRS-7, Uetikon-Zuerich, Switzerland; Transactions Technology Publications Ltd, 2005: 311-316.

[12] 江克斌, 肖叶桃, 郭永涛. T形焊接试件焊接残余应力分布的测定[J]. 焊接学报, 2008, 29(1): 53-56.  
Jiang Kebin, Xiao Yetao, Guo Yongtao. Welding residual stress determination of T-welded specimens the distribution[J]. Transactions of the China Welding Institution, 2008, 29(1): 53-56.

[13] Makoto H, Kunio E. Changes in residual stress in worked surface layer of type 304 austenitic stainless steel due to tensile deformation[J]. Journal of Pressure Vessel Technology, 2001, 123(1): 130-134.

[14] 陈怀宁, 陈亮山, 林泉洪. 逆焊接加热处理引入压缩残余应力的数值分析[J]. 机械强度, 2002, 24(1): 73-76.  
Chen Huaining, Cheng Liangshan, Lin Quanhong. Numerical analysis of compressive residual stress induced by anti-welding-heating treatment[J]. Journal of Mechanical Strength, 2002, 24(1): 73-76.

[15] 徐东, 宋天民, 张国福, 等. 逆焊接处理对金属材料抗疲劳性能的测试[J]. 辽宁石油化工大学学报, 2007, 27(3): 38-40.  
Xu Dong, Song Tianmin, Zhang Guofu, et al. Test on fatigue resistance ability of metallic materials based on anti-welding-heating treatment[J]. Journal of Liaoning University of Petroleum & Chemical Technology, 2007, 27(3): 38-40.

作者简介: 张亦良, 女, 1955 年出生, 大学本科, 教授. 研究方向为试验力学、疲劳断裂、材料应力腐蚀、结构件残余应力、失效分析及安全评定等. 发表论文 100 余篇.

Email: zhangyil@ljut.edu.cn

**Abstract:** In order to improve the welding efficiency, triple-electrode high-speed CO<sub>2</sub> fillet welding process was adopted based on the twin-electrode CO<sub>2</sub> welding and the effect of welding conditions on weld geometry parameters was analyzed. The results show that weld geometry parameters are more or less the same by DCEP/DCEN/DCEP and DCEN/DCEP/DCEN polarities. Leg length, penetration and weld width increase with the speed slowdown and welding combination parameters increase, but leg length has a maximum limit. Middle-electrode offset plays an important role in welding geometry parameters and the leg length is the smallest when the electrodes shift from one side to the other side is  $\pm 30$ mm in this experiments. In addition, the leg length and weld width gradually decrease with increasing the distance of wire to wire.

**Key words:** triple-electrode high speed CO<sub>2</sub> fillet welding; polarities; electrodes shift; weld geometry parameters

#### Elimination and evaluation of welding residual stress in sterilizers welded by combined process

ZHANG Yiliang<sup>1</sup>, LIU Jinyan<sup>1</sup>, ZHAO Ebing<sup>2</sup>, XU Xuedong<sup>1</sup>, CHENG Hongwei<sup>2</sup> (1. Beijing University of Technology, Beijing 100124, China; 2. Chaoyang Special Equipment Inspection Institute of Beijing, Beijing 100021, China). p 97–101

**Abstract:** Observing that cracks appear simultaneously on multi-location near weld on intracavity of domestic vacuum, we investigate a series of studies on welding residual stress and its corresponding elimination methods. We design seven types of combined-structure plates and quantitatively measure the residual stress distribution by X-ray method based on the characteristics of discontinuous welding of different steel in sterilizers. The results show that welding residual stress of all seven types of boards reaches yield stress and causes the stress corrosion and corrosion fatigue which are main reasons of the intracavity cracking of sterilizers. In addition, residual stress resulted from carbon dioxide welding is 10%–22% higher than manual welding, and residual stress is indifferent with rebar type. After experimental verification of post-welding watering quick-cooling technology to eliminate the residual stress, we conclude that watering quick-cooling can effectively reduce the surface residual stress by 50%–70% and increase fatigue limit by 12%–14% on watering surface. Reducing welding residual stress is an important way to solve the problem of cracking in the intracavity of sterilizers.

**Key words:** weld; residual stress; X-ray method; sterilizer; crack

#### Character analysis of negative polarity weak plasma arc overlaying welding

LIU Zhengjun, YANG Yang, ZHAO Qian, ZHANG Shixin (School of Material Science and Engineering, Shenyang University of Technology, Shenyang 110178, China). p 102–104

**Abstract:** The essential characteristics of overlaying welding, the influence of the flow and content of protective air on energy density, the arc radial pressure distribution, the heat distribution of plasma arc, the combustion stability and static characteristic of nega-

tive polarity weak plasma arc are analyzed. The results indicate that the arc pressure of negative polarity weak plasma arc is homogeneous, the radial distribution graph of arc voltage, the radial distribution graph of arc current and the distribution area of cathode spot all have saucer shape, the energy of cathode spot takes up 50% than that of the effective energy, 90% of the current distributes in the annular area of internal diameter of 10 mm, and changing the flow capacity of protective air can control energy density. The cathode atomising action of negative polarity weak plasma arc can effectively improve the combine condition of overlaying metal and basal metal, which makes negative polarity weak plasma arc be one of the perfect thermal resource at dissimilar material overlaying welding.

**Key words:** negative polarity; weak plasma arc; arc energy; arc pressure

#### In-situ detection of weld metal thermal cycle of 10CrMo910 steel

HU Yanhua, CHEN Furong, XIE Ruijun, LI Haitao (College of Materials Science and Engineering, Inner Mongolia University of Technology, Hohhot 010051, China). p 105–107

**Abstract:** 10CrMo910 steel was welded by using proper parameters for solving the problem of cold crack and local hardening in the weld or adjacent metal weld of 10CrMo910 steel. Thermo-couples were laid in welded seam during welding to record temperatures in situ, and in-situ detection of thermal cycle about weld metal was realized. The detected maximum temperature during thermal process was 1701 °C and above 401 °C than the reported results about heat-affected zone. The welding thermal cycle curves with oil-cooled, air-cooled and sand-cooled for different cooling rates of welded joint were obtained.

**Key words:** weld metal; welding thermal cycle; in-situ detection

#### Research status analysis of electron beam welding for joining of dissimilar materials

FENG Jikai, WANG Ting, ZHANG Binggang, CHEN Guoqing (State Key Laboratory of Advanced Welding Production Technology, Harbin Institute of Technology, Harbin 150001, China). p 108–112

**Abstract:** Electron beam welding (EBW) in the field of joining dissimilar materials has been a subject of interest in recent years based on special features of EBW, e. g. high energy density, accurately controllable beam size and location, low residual stress and pollution-free weld. Numerous successful results have been achieved, and some of them have already been exploited in industrial production. Since EBW is a fusion welding method, difficulties associated with metallurgical phenomena still exist. This paper is aimed to have an analysis of the research status of electron beam welding for the joining of dissimilar materials. A summary of the existing problems and solutions during electron beam welding of different type of dissimilar material joint has been conducted and the key points of research in future are also proposed.

**Key words:** dissimilar materials; electron beam welding; research status